Journal of Morphology

WILEY

JOURNAL OF morphology

RESEARCH ARTICLE

Anatomy of the Critically-Endangered Anji Salamander (*Hynobius amjiensis*) Provides New Insights Into Morphological Evolution of Salamanders

Cang-Song Chen[1] | Jia Jia[2] | Xian-Ting Wang[3] | Jia Yang[1] | Ke-Qin Gao[4]

[1]Zhejiang Museum of Natural History, Hangzhou, Zhejiang Province, China | [2]Institute of Vertebrate Paleontology and Paleoanthropology, Chinese Academy of Sciences, Beijing, China | [3]Anji Salamander National Natural Reserve Management Center, Huzhou, Zhejiang Province, China | [4]School of Earth and Space Sciences, Peking University, Beijing, China

Correspondence: Jia Jia (jiajia@ivpp.ac.cn) | Ke-Qin Gao (kqgao@pku.edu.cn)

Received: 2 December 2024 | **Revised:** 13 January 2025 | **Accepted:** 18 January 2025

Funding: This research was supported by the National Natural Science Foundation of China (NSFC 41872008, 41702002) and the Natural Science Foundation of Zhejiang (LTGS23C030003 and LGN19C040002).

Keywords: anatomy | critically-endangered species | *Hynobius amjiensis* | middle ear | ontogeny and phylogeny

ABSTRACT

The Anji Salamander (*Hynobius amjiensis*) is a critically-endangered amphibian endemic to the Tianmushan Mountain area in southeastern China. As most of its congeneric species in the ancestral salamander family Hynobiidae, the osteology of *H. amjiensis* has remained essentially unknown and has hampered efforts in understanding morphological evolutionary patterns of early salamanders. Here, we investigate the skeletal anatomy of *H. amjiensis* based on microcomputed tomography scans of post-metamorphosed juvenile and adult specimens. Our results reveal Hynobiidae has more early-tetrapod-like plesiomorphic characters than expected, as *H. amjiensis* has a stapedial foramen in the middle ear and two centralia and a centrale-radius contact in the limb. We demonstrate that *Hynobius amjiensis* is the first known living salamander species with a stapedial foramen whose absence was believed to unite salamanders and anurans, and hence opens major questions on the evolution of the middle ear in modern amphibians: if some salamanders and caecilians had a stapedial foramen inherited from their common ancestor, when and how many times was the foramen lost independently in modern amphibians, and how did this structural loss impact the phylogenetic evolution of salamander clades? Our findings of hyper-ossified pectoral and pelvic girdles and loss of postminimus in the pes in *H. amjiensis* demonstrate that functional morphological features in hynobiids are potentially informative in phylogeny and ontogeny of early salamanders.

1 | Introduction

Hynobiidae, or Asiatic Salamanders, has 98 living species in 10 genera, and constitutes the majority of the most primitive living salamander suborder Cryptobranchoidea (AmphibiaWeb 2024). To date, hynobiids are the only living salamander group with fossil record dated back to the Middle Jurassic (~166 Ma), as several stem hynobiids were discovered from the Yanliao Biota at northern China (Jia, Anderson, and Gao 2021a). Hynobiids are essential in understanding the early evolution of salamanders, as they have many plesiomorphic characters that are evolutionarily lost in derived groups, such as external fertilization and presence of microchromosomes. Hynobiids are also valuable in understanding the evolution of early tetrapods for the presence of transitional/atavistic characters such as supernumerary caudosacrals and centralia in carpus/tarsus (Jia, Anderson, and Gao 2021a; Jia et al. 2022). The ancestral characters prompt some studies to claim hynobiids as a

paraphyletic basal group from which derived salamander groups originate (Trueb 1993; Boisvert 2009), though the monophyletic status of Hynobiidae is strongly supported in molecular cladistic analyses (Zhang et al. 2006; Chen et al. 2015). Fortunately, a growing body of osteological studies on living hynobiids augment our knowledge of morphological evolutionary patterns of this long-lasting clade, for example, several synapomorphies (e.g., presence of anteroventral process of orbitosphenoid) of crown-group hynobiids are found when investigating the osteology of a major living derived hynobiid clade endemic to southwestern China including *Batrachuperus*, *Liua*, *Protohynobius*, and *Pseudohynobius* (Jiang et al. 2018; Jia et al. 2019; Jia, Anderson, and Gao 2021a; Jia et al. 2021b). By contrast, osteology of the other deeply-nested hynobiid clade, *Hynobius*, is poorly studied (Sato 1943; Xiong, Liu, and Zeng 2011; Vassilieva et al. 2015; Hara and Nishikawa 2021).

Hynobius is the most specious genus in Hynobiidae that includes ~ 66% living hynobiids distributed in Japan (47/65), eastern China (12/65), Korea (6/65), and Central Asia (1/65; AmphibiaWeb 2024). In China, five *Hynobius* species are found endemic to Taiwan with relatively wide distribution ranges at high altitudes (1300–3650 m above sea level), whereas six endemic *Hynobius* species in southeastern mainland China are primarily distributed with restricted ranges at low altitudes (50–2015 m; Sparreboom 2014; Fei and Ye 2016), and most of the latter hynobiid salamander species are critically endangered, including *H. amjiensis*, *H. bambusicolus*, *H. guabangshanensis*, and *H. maoershanensis*.

The Anji Salamander (*Hynobius amjiensis*) is only found from the type locality Longwangshan (1300 m) in Zhejiang Province, China (supplementary online material Figure S1), and neighboring Qingliangfeng on both the Anhui (1450 m) and Zhejiang (1600 m) sides of the provincial border (Gu 1992; Li et al. 2013; Chen et al. 2016; IUCN SSC Amphibian Specialist Group 2021). At the type locality, *H. amjiensis* inhabits marshy meadow environments covered with peat moss of the genus *Sphagnum*, and it was reported that the salamander can only be spotted during breeding season (November through March; Gu et al. 1999; Chen and Yang 2012; Li et al. 2013; Chen et al. 2016). The Anji Salamander is listed as critically endangered in the IUCN Red List and in the Red List of China's Vertebrates (IUCN 2007; IUCN 2019; Jiang et al. 2016), because its population represented by breeding females in natural habitats is declined from ~260 (at Longwangshan) in 1999 (Gu et al. 1999) to 121 (at Longwangshan) and 95 (at Qingliangfeng) in 2013 and 2014 combined due to habitat destruction (Chen et al. 2016). To protect *H. amjiensis*, many aspects of its biology have been extensively studied including ecological adaptation, population genetics, and embryonic development (Gu et al. 1999; Fu et al. 2003; Chen et al. 2016; Yang et al. 2016; Chen et al. 2023; Cao et al. 2024; Qiu et al. 2024), and it was found to be the sister taxon to the newly-discovered *H. bambusicolus* from Fujian Province (Wang et al. 2023). However, the anatomy of *H. amjiensis* remains unknown even though it has been known by the scientific community for 33 years (Gu 1992). Here, we present results of our investigation of the osteological morphology of the Anji Salamander based on microcomputed tomography (micro-CT) scans. A mosaic of derived and more atavistic characters in the middle ear and limb structures are found and are discussed with the aim to better understanding morphological evolution of salamanders.

2 | Materials and Methods

2.1 | Sampled Specimens

Seven wet preserved specimens (four adults and three juveniles) of *Hynobius amjiensis* Gu 1992 were used in this study (supplementary online material Table S1). The specimens are preserved in 10% formaldehyde solution, cataloged in the collections of the Zhejiang Museum of Natural History, Hangzhou, Zhejiang Province, China. All specimens are post-metamorphosed because larval features such as external gills, gill slits or high caudal fin are lost. Adults were distinguished from juveniles primarily by ossifications in carpals and tarsals, which ossify long after sexual maturity is reached in salamanders (Jia et al. 2022), and were supplemented by reduction or complete closure of the anterodorsal fenestra in the skull roof. Morphological descriptions below are based on all seven specimens with intraspecific variations noted whenever observed.

2.2 | Micro-CT Scans

The specimens were whole-body scanned along the sagittal axis using a Nikon XT H320 LC scanner at Zhejiang University in Hangzhou. Scanning of the specimens was performed at a voltage of 120–160 kV and a current of 100–120 μA. The usage of regular high-resolution microcomputed tomography allows us to study and focus on the osteology of the critically-endangered Anji Salamander without bringing any destructions to the valuable specimens, and any attempts to study cartilages can be achieved by using contrast-enhanced CT scans in the future. Segmentation, rendering and measurement were made by using VG Studio Max 2.2 (Volume Graphics, Heidelberg, Germany). Anatomical structures were labeled using Adobe Photoshop CS6 (San Jose, California, USA).

2.3 | Institutional Abbreviations

FMNH, Field Museum of Natural History, Chicago, Illinois, USA; **HTC**, Hangzhou Teachers College (Hangzhou Normal University), Hangzhou, Zhejiang Province, China; **ZMNH**, Zhejiang Museum of Natural History, Hangzhou, Zhejiang Province, China.

3 | Results

3.1 | Systematic Zoology

Order Urodela Duméril (1806)

Suborder Cryptobranchoidea Dunn (1922)

Family Hynobiidae Cope (1859)

Genus *Hynobius* Tschudi (1838)

Species *Hynobius amjiensis* Gu (1992)

3.2 | Holotype

HTC 90301, an adult male with a total length of 166 mm.

3.3 | Type Locality

Longwangshan (E119°27.32', N30°23.68'), ~60 km northwest of Hangzhou, Zhejiang Province, China (supplementary online material, Figure S1).

3.4 | Diagnosis

Distinguished from other congeneric species by the following osteological features in the adult: anterodorsal fenestra fully closed by a mid-line contact of premaxillae and nasals; lacrimal posteriorly entering rim of orbit; maxillary tooth row terminating a short distance from posterior extremity of maxilla; vomerine tooth row inverted L-shaped with a long medial ramus extending posteriorly to mid-level of orbit; anteromedial fenestra large; articular remaining cartilaginous; basibranchial II reduced as a transverse bar with a tiny median process; tail slightly shorter than snout-vent length, with two-to-three caudosacrals and maximal 30 caudals; procoracoid and scapulocoracoid co-ossified; intermedium fused with ulnare; proximal centrale in direct contact with radius; metacarpal II expanded anteroposteriorly; pubis partially ossified and fused with ischium; presence of two centralia but lost postminimus in pes.

3.5 | Anatomical Description

Medium-sized salamander with a total body length of 136.16–167 mm in the adult (Chen et al. 2016; Fei and Ye 2016). The head is flat, with a blunt and round snout. The eyes pop up prominently from the surface of the head. A lip fold is absent, and both nuchal and gular folds are present. The trunk in the adult is stout and cylindrical, with 13 costal grooves. The tail is bilaterally compressed, slightly shorter than the snout-vent length. The manus has four fingers, and the pes has five toes.

3.5.1 | Skull and Mandible

The skull is subtriangular with a rounded snout. An anterodorsal fenestra is observed in juvenile specimens (ZMNH AA872–AA874), but is fully closed by a midline contact of the nasals in fully-grown adults (e.g., ZMNH AA868; Figure 1B).

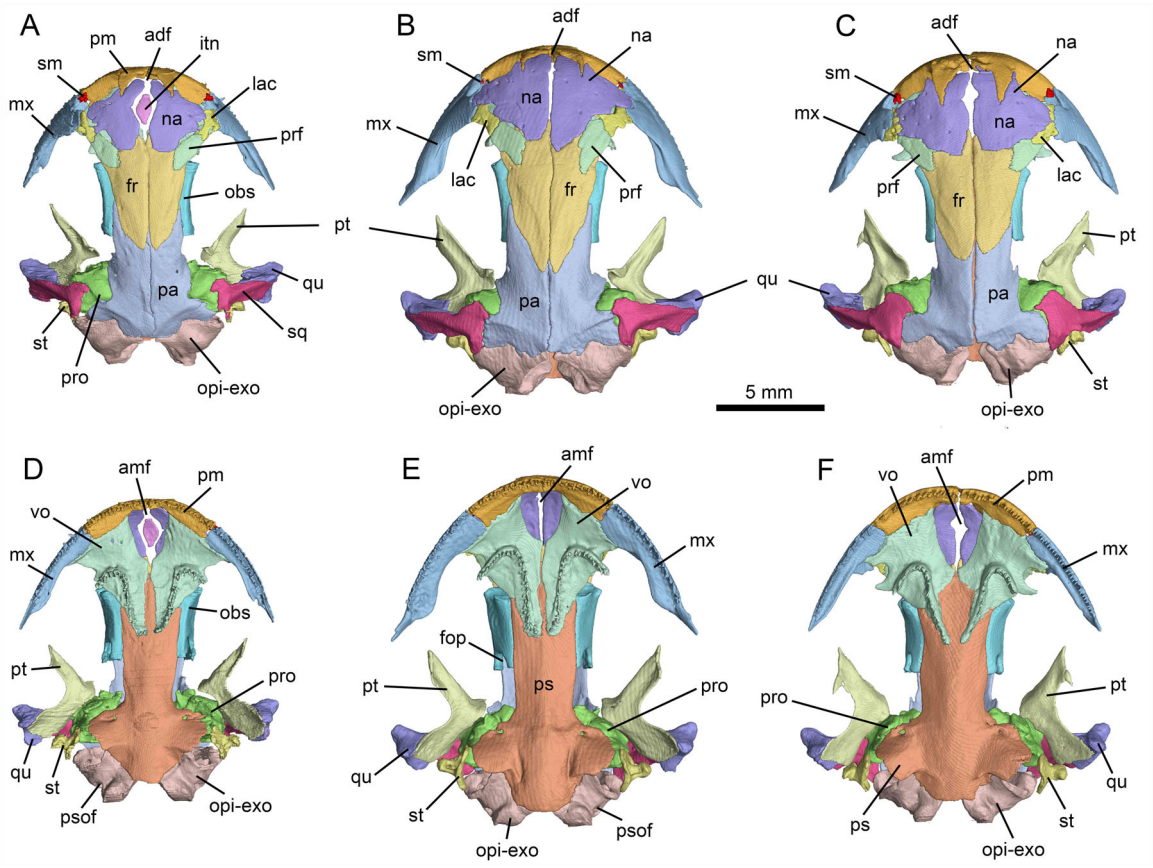

FIGURE 1 | Micro-CT rendered reconstruction of the skull of *Hynobius amjiensis* in dorsal (above) and palatal (below) views. (A, D) ZMNH AA869; (B, E) ZMNH AA868; (C, F) ZMNH AA870. Abbreviations: adf, anterodorsal fenestra; amf, anteromedial fenestra; fop, foramen opticum; fr, frontal; itn, internasal; IX + X, foramen for combined nervus glossopharyngeus (IX) and vagus (X); lac, lacrimal; mx, maxilla; na, nasal; obs, orbitosphenoid; opi-exo, opisthotic-exoccipital complex; pa, parietal; pm, premaxilla; prf, prefrontal; pro, prootic; ps, parasphenoid; pt, pterygoid; qu, quadrate; sm, septomaxilla; sq, squamosal; st, stapes; vo, vomer.

An internasal bone is variably present in some (e.g., ZMNH AA869; Figure 1A,D) but not all specimens.

The paired bony nasals are separated by the anterodorsal fenestra in juveniles and young adults, and approach closely to each other along a midline suture with an extreme narrow fissure in between in fully-grown adults. The lateral expansion of the nasals is wider than the width of the frontals as in other hynobiids (Dunn 1922; Gao and Shubin 2012). In fully-grown adults, the lateral process of the nasal contacts the pars facialis of the maxilla over the lacrimal (Figure 1B). The septomaxilla is ossified within the external naris, immediately above the anterior process of the maxilla. The septomaxilla is scrolled to form a tube supporting the nasolacrimal duct, and also serves as the origin of the muscularis dilatator/constrictor naris for respiratory currents control (Wilder 1925; Lapage 1928).

The paired frontals meet along a midline suture. The widened anterior end of the frontal is in contact with the nasal and prefrontal, but not with the lacrimal. The lateral edge of the frontal slightly curves downward to articulate with the orbitosphenoid. Posteriorly, the frontal has a tongue-like process overlapping the parietal along the midline suture. The paired parietals form a large skull table. The parietal is roughly "L"-shaped with a posterolateral boot in contact with the squamosal (Figure 1B,C). Anterior to the lateral boot, the parietal is penetrated by a small foramen, through which passes the trochlear nerve (CN IV). The lacrimal is set between the nasals and maxilla, and between the external naris and the orbit. However, the lacrimal in fully-grown adults is anteriorly covered by the lateral process of the nasal, so it does not enter the rim of the external naris in dorsal view. The lacrimal canal opens on the posterodorsal surface and runs through the lacrimal anteroventrally into the nasal cavity.

The pars facialis of the maxilla contacts both the nasal and lacrimal (Figure 1 and S2). The posterior process of the maxilla extends to the midlevel of the orbit, where it connects with the pterygoid by a ligament. In palatal view, the pars palatina of the maxilla forms a narrow shelf, the anterior part of which is medially in articulation with the vomer. The prefrontal is a short plate that forms the anteromedial rim of the orbit between the frontal and lacrimal. Anteriorly, it has a sutural contact with the nasal and lacrimal, but not with the maxilla.

The squamosal is "T"-shaped, having an expanded proximal end in articulation with the parietal and a strip-like lateral process sloping towards the cranio-mandibular joint. The proximal end bears a robust anterior process above the otic capsule and a posterior process contacting the opisthotic-exoccipital complex. The quadrate is dorsally concealed by the squamosal, except for its expanded distal end exposed beyond the squamosal. The ascending process of the quadrate extends toward the otic region (supplementary online material, Figure S2), where it connects by a ligament with the stapes (Kingsbury and Reed 1908; Kingsbury and Reed 1909). The distal end of the quadrate has a saddle-shaped articular surface for the cranio-mandibular joint. Also at the distal end, a small quadrate foramen opens for passage of the posterior condylar artery and vein (Olson 1966). A large posterior process of the quadrate indicates a strong ligamentous connection with the cartilaginous ceratohyal (Kingsbury and Reed 1908).

The pterygoid is triradiate, with its elongate palatal and quadrate processes angled at 90 degrees. The palatal process is dorsally grooved to hold the cartilaginous rod of the pterygoid process of the palatoquadrate. The quadrate process is a thin blade, extending posterolaterally to reinforce the suspensorium. In addition, a short otic process of the pterygoid projects dorsomedially anterior to the prootic. Above the otic process, the ascending process of the palatoquadrate is not ossified, in contrast with some other hynobiids (Jiang et al. 2018; Jia et al. 2019).

The paired vomers are widely separated by a large anteromedial fenestra in the anterior part, approach closely to each other with an extreme narrow median suture in the middle part and are diverged laterally again in the posterior part. The lateral border of the vomer is notched for the choana anterolateral to the vomerine tooth row. The posterior process of the vomer extends posteriorly during development and terminates to the mid-level of the orbit in adult specimens; thus, it covers much of the anterior part of the parasphenoid. The parasphenoid is a large median element that floors the braincase. The posterior part of the parasphenoid is strongly widened, with wing-like lateral alae flooring the otic capsules. A pair of foramina perforate the lateral wings for the passage of the internal carotid artery.

The orbitosphenoid is a rectangular plate in lateral view, forming the interorbital walls of the braincase. The dorsal edge of the element contacts both the frontal and parietal, whereas its ventral edge articulates with parasphenoid and vomer (Figure 1 and supplementary online material Figure S2). Anteriorly, the orbitosphenoid is slightly notched for the border of the orbitonasal fenestra, and its posterior border is deeply notched for the foramen opticum (Figure 1). A subtriangular anteroventral process extends over the parasphenoid from the ventromedial border of the orbitosphenoid (Figure S2) as in other living hynobiids.

The prootic forms the anterolateral wall of the otic capsule anterior to the fenestra ovalis (Figure 1, S2). In dorsal view, the alary process of the prootic is exposed in a V-shaped cleft between the parietal and squamosal. In ventral view, the prootic is penetrated by a small foramen palatinum, through which passes the ramus palatinus of the nervus facialis (CN VII; Francis 1934). Posterolateral to this foramen opens a much larger foramen faciale as the passage of the truncus hyomandibularis of the nervus facialis (CN VII) (Francis 1934). The posterior border of the prootic is notched for the anterior rim of the fenestra ovalis.

The disc-like footplate of the stapes covers the fenestra ovalis; a short stylus is fused with the footplate. A stapedial foramen is clearly present in both juveniles and adults (Figure 2; S2). No operculum is ossified in any specimens, but a triangular gap immediately ventral to the fenestra ovalis indicates the presence of a cartilaginous operculum, the origin of M. levator scapulae (Gregory, Peabody, and Price 1956; Monath 1965).

The opisthotic is fused with the exoccipital to form an opisthotic-exoccipital complex (Figures 1 and 2, S2). The exoccipital portion of the complex bears the occipital condyle for articulation with the atlas. Laterally at the base of the condyle, the foramen post-oticum opens for passage of the combined

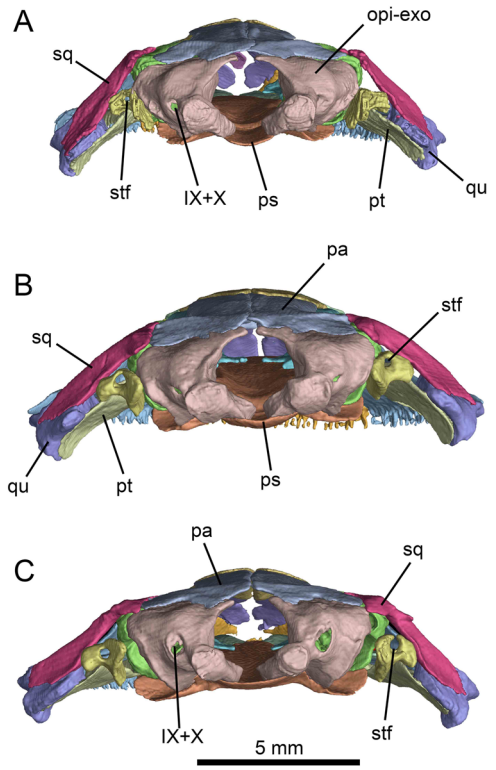

FIGURE 2 | Micro-CT rendered reconstruction of the skull of *Hynobius amjiensis* in occipital view to show the stapedial foramen. (A) ZMNH AA869; (B) ZMNH AA868; (C) ZMNH AA870. Abbreviations: IX + X, foramen for combined nervus glossopharyngeus (IX) and vagus (X); opi-exo, opisthotic-exoccipital complex; pa, parietal; ps, parasphenoid; pt, pterygoid; qu, quadrate; sq, squamosal; stf, stapedial foramen.

nervus glossopharyngeus and vagus (CN IX and X). Above the foramen magnum, the opisthotic-exoccipital complex approaches but does not meet its counterpart, leaving a small gap filled by the cartilaginous tectum synoticum.

In the mandible, ossified elements include the dentary, prearticular, angular, and a mentomeckelian fused with the dentary as a posterior mental process at the symphysis (supplementary online material, Figure S3). A bony articular is not observed in the juvenile or the adult; thus, it may remain cartilaginous as indicated by a large gap between the prearticular and dentary posterodorsally in the mandible. The dentary is the only tooth-bearing element in the mandible. The lateral surface of the dentary is penetrated by several mental foramina (Figure S3), through which pass the cutaneous branches of the ramus mandibularis (CN V_3). The prearticular covers most of the inner aspect of the mandible, with its anterior extension extending to the midlevel of the dentary tooth row. Posterodorsally, the prearticular carries a large coronoid process for the insertion of the M. levator mandibulae (Carroll and Holmes 1980). Posteroventral to this process, the prearticular is penetrated by the inferior dental foramen (Figure S3), the passage of the ramus alveolaris of the nervus facialis (CN VII) and its associated alveolar artery. The angular is a small splint posteroventrally wedged between the prearticular and dentary. Medially close to the anterior end of the angular, the angular foramen opens as the passage for a branch of the nervus trigeminus (CN V_3; Francis 1934).

3.5.2 | Dentition

Both marginal and vomerine teeth are pedicellate with bicuspid crowns. All marginal teeth are pleurodont, whereas the vomerine teeth are ankylosed to the ventral surface of the vomers. The premaxillary tooth row contains 18–20 teeth; the maxillary tooth row contains up to 30 teeth. The vomerine tooth tow forms an inverted "L", with the medial ramus elongated as more than twice the length as the lateral ramus (Figure 1). The two rami are roughly equal in length in the juvenile, but the medial ramus in the adult becomes much extended, along with the posterior extension of the vomerine process as an ontogenetic feature. The dentary tooth row contains 45–50 teeth. It extends from the mandibular symphysis to the midlevel of the mandible, where the coronoid process of the prearticular begins its ascent (Figure S3).

3.5.3 | Hyobranchial Apparatus

In post-metamorphic juveniles, hypobranchial II is fully ossified whereas ceratobranchial II is not yet or only partly ossified (supplementary online material, Figure S4). This delayed ossification is different from the Taiwan Salamander (*Hynobius formosanus*), in which the ceratobranchial II ossifies before metamorphosis (Vassilieva et al. 2015). In adults, both hypobranchial II and ceratobranchial II are ossified as elongate rods (Figure 3). Hypobranchial II curves posterolaterally, whereas ceratobranchial II curves posterodorsally. Basibranchial II is ossified as an inverted "T" in juveniles, but the short anterior stem is reduced as a tiny stub and the transverse bar is elongated in adults.

3.5.4 | Axial Skeleton

The axial skeleton consists of the atlas, 15 or 17 rib-bearing trunk vertebrae, a single sacral, followed by two-to-three caudosacrals and up to 30 caudals (Figure 3, supplementary online material Figures S4, S5). The atlas is laterally penetrated by a foramen for the first pair of vertebral nerves. A robust interglenoid tubercle projects anteroventrally to reinforce the cotylecondylar articulation of the vertebral column with the skull. Lateral to the interglenoid tubercle are the paired atlantal cotyles articulating with the occipital condyles.

The trunk vertebrae are similar in length, each dorsally carrying a low neural spine for attachment of the M. interspinalis (Vassilieva et al. 2015). The centrum is cylindrical and deeply amphicoelous. All trunk vertebrae bear a pair of unicapitate ribs. The ribs associated with the anterior three trunk vertebrae are more robust than the others, with a spatulate distal end for attachment of the M. thoracicscapularis (Francis 1934). The third rib often carries an uncinate process.

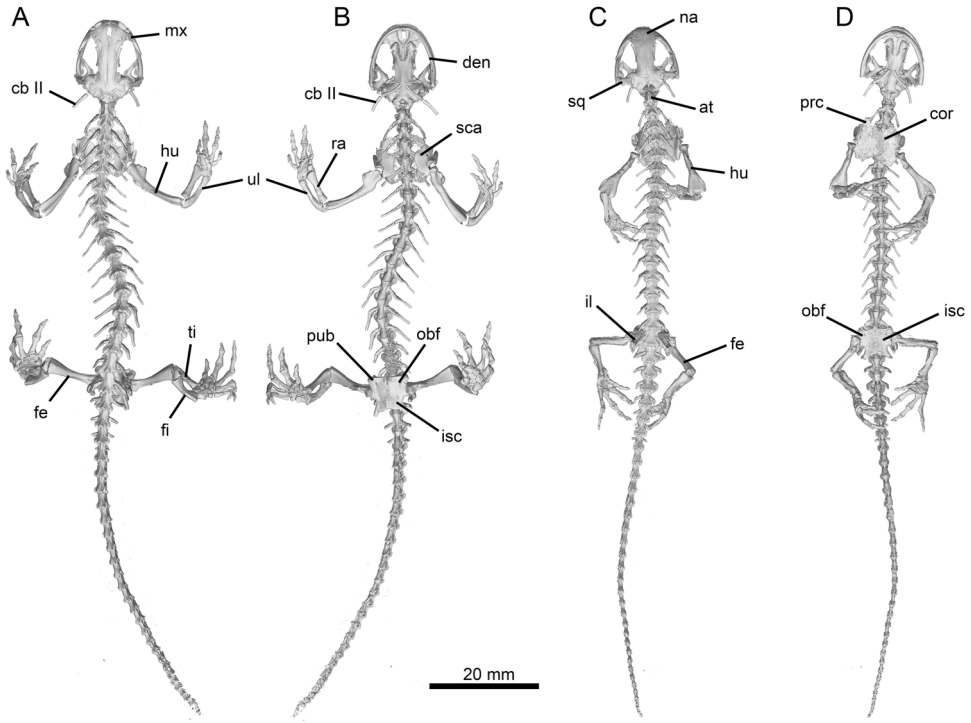

FIGURE 3 | Micro-CT rendered reconstruction of whole-body skeleton of *Hynobius amjiensis* in dorsal and ventral views: (A, B) ZMNH AA871 (note this young adult displays complete fusion of pubis with ischium in the pelvic, while the procoracoid and coracoid have just started to ossify in the shoulder); (C, D) ZMNH AA868 (note this fully-grown adult displays the most extensive fusion of elements in both pectoral and pelvic girdles). Abbreviations: an, angular; at, atlas; cb, ceratobranchial; cor, coracoid; den, dentary; fe, femur; fi, fibula; hb, hypobranchial; hu, humerus; il, ilium; isc, ischium; mx, maxilla; na, nasal; obf, obturator foramen; prc, procoracoid; pub, pubis; ra, radius; sca, scapulocoracoid; sq, squamosal; ti, tibia; ul, ulna.

The sacral is similar to the trunk vertebrae, except for having transverse processes and ribs that are more robust than those of the trunk series. The first few caudosacrals bear ribs, and the last caudosacral bears the first hemal spine in the post-sacral vertebrae. The true caudal series consists of 28–30 vertebrae in adults (Figure 3, S4 and S5). Only the first one or two caudals bear ribs. Ventrally, the hemal spine of the first caudal characteristically bends posteriorly at an angle greater than 90 degrees. The hemal spine becomes shorter posteriorly, and eventually vanishes in the last five caudals.

3.5.5 | Appendicular Skeleton

The scapulocoracoid is ossified as a single unit in the juvenile (supplementary online material Figure S4). The coracoid part of the scapulocoracoid is expanded anteroposteriorly with its ventral border grooved for articulation with the cartilaginous procoracoid and coracoid. However, extra ossification of the pectoral girdle is found in the procoracoid and in the coracoid plate ventromedial to the coracoid part of the scapulocoracoid in fully-grown adults (Figure 3D, S5). Anteroventral to the glenoid fossa opens the foramen supracoracoideum, the passage of the nervus supracoracoideus and its associated vessels.

The humerus has a large head, short and constricted shaft, but expanded proximal and distal ends. On the extensor side, a prominent tubercle of the crista dorsalis humeri marks the insertion of the M. subscapularis. On the flexor side, the humeral head merges with the large crista ventralis humeri, onto which insert the MM. pectoralis and supracoracoideus (Vassilieva et al. 2015). Distally on the flexor side is the fossa cubitalis ventralis, which receives the proximal end of the radius when the forearm is flexed. The ulna is slightly longer than the radius (Figure 4). The postaxial side of the radius bears a prominent tubercle for ligamentous insertion of the elbow flexor M. humeroantibranchialis, whereas a crest on the posterolateral side of the ulna marks the insertion of the M. extensor antibrachii ulnaris (Vassilieva et al. 2015).

The fully ossified manus displays eight carpal elements. The intermedium is fused with the ulnare, a derived feature in salamanders. Two centralia are present, with the proximal centrale contacting the radius, an atavistic feature in salamanders (Shubin and Wake 2003; Figure 4). The radiale is large, distally in contact with the element y, which is one-half the size of the former. The basale commune is a large element distally in articulation with metacarpals I and II. Distal carpals 3 and 4 are roughly the same size, and distally in articulation with metacarpals III and IV, respectively. Metacarpal II is enlarged anteroposteriorly. The manus displays a phalangeal formula of 2-2-3-2, a generalized pattern in salamanders (Figure 4).

The ilia and ischia of the pelvis are ossified in post-metamorphic juveniles, but in addition ossification of the pubes occurs in

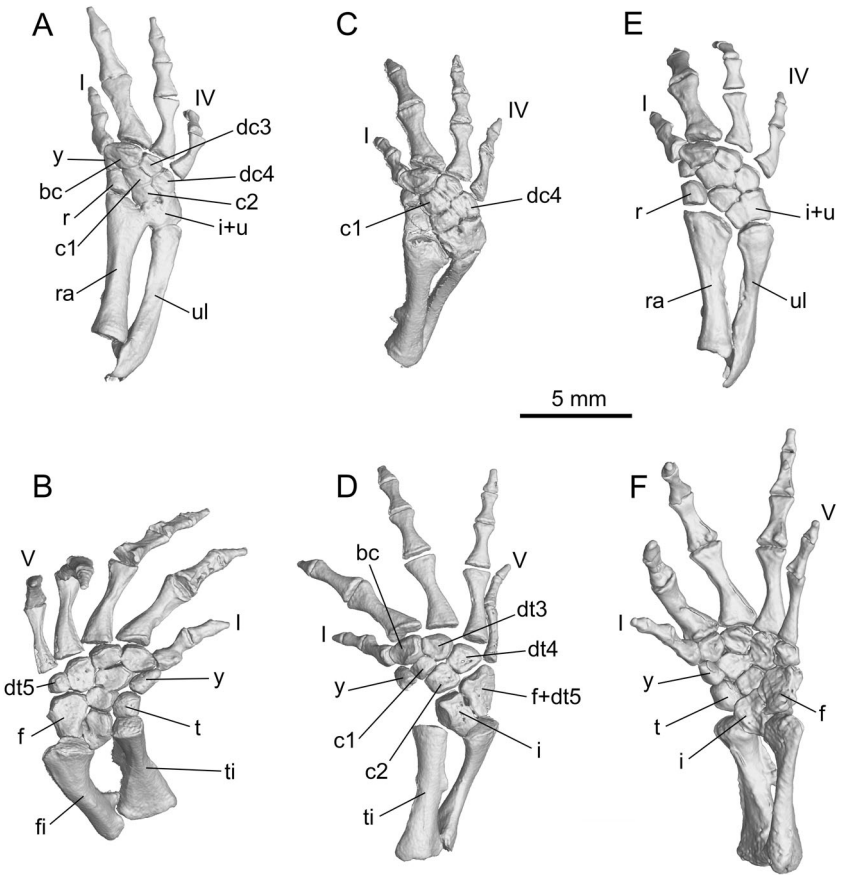

FIGURE 4 | Micro-CT rendered reconstruction of the carpus (A, C, E) and tarsus (B, D, F) of *Hynobius amjiensis* in dorsal and ventral views: (A, B) ZMNH AA871; (C, D) ZMNH AA869; (E) ZMNH AA870; (F) ZMNH AA868. Note a large basal centrale in direct contact with the radius. Abbreviations: bc, basale commune; c, centrale; dc, distal carpal; dt, distal tarsal; f, fibulare; fi, fibula; i + u, intermedium-ulnare; r, radiale; ra, radius; t, tibiale; ti, tibia; ul, ulna; y, element y.

adults. The ypsiloid is not ossified in both the juvenile and adult specimens. The ilium is a robust club, with a thick blade and slightly expanded ventral base contributing a small part to the acetabulum. In the adult, the ischium and pubis are fused to form a large pubo-ischium, which is anteriorly perforated by the small obturator foramen (Figure 3B,D, supplementary online material Figure S5). The pubo-ischium posterolaterally bears a robust ischial spine, onto which attaches the M. ischio-caudalis as the flexor of the tail.

The femur has a large head, fitting into the acetabulum. On the extensor side, the dorsal trochanteric crest extends from the femoral head to the fibular condyle along the post-axial border of the femur. It marks the insertion of the M. pubo-ischio-femoralis internus, a powerful extensor of the upper leg in salamanders (Francis 1934). Proximally on the flexor side, a twig-like process marks the femoral trochanter, on which inserts the M. pubo-ischio-femoralis externus (Ashley-Ross 1992). Posterior to the trochanter is the trochlear groove, which receives the ischial process at the ventral rim of the acetabulum when the leg swings backwards. The tibia and fibula are similar in length, being over half the length of the femur. Both the tibia and fibula are robust, having expanded proximal and distal ends with slightly constricted middle shaft, but the tibia is more expanded proximally than distally, and the fibula is more expanded distally than proximally. The tibia bears a prominent crest postaxially for the insertion of the M. extensor cruris tibialis (Ashley-Ross 1992).

Maximum ossification of the tarsus displays ten tarsals in fully-grown adults. The intermedium is diamond-shaped, proximally wedged between the tibia and fibula. The tibiale as a preaxial element is the last to become ossified. The fibulare is larger than the tibiale or intermedium. Two centralia are present, as in the manus. Among the distal tarsals, element y is ossified before the tibiale; this ossification sequence is the same as in the Longdong Stream Salamander (*Batrachuperus londongensis*; Jiang et al. 2018), but differs from the Yenyuan Stream Salamander (*Batrachuperus yenyuanensis*), in which the tibiale is ossified before element y (Jia et al. 2019). The basale commune is twice the size of element y. Distal tarsals 3 and 4 are similar in size, whereas the postminimus is absent (Figure 4). Loss of the postminimus has been recognized as a derived condition in salamanders (Shubin and Wake 2003). More distally, metatarsals III and IV are subequal in length, whereas metatarsal II is slightly longer than V, and I is the shortest. The five digits display a relative length of $3 > 4 > 2 > 5 > 1$. The phalangeal formula is 2-2-3-3-2, a generalized pattern in salamanders.

4 | Discussion

Our studies of the Anji Salamander based on micro-CT scan of seven specimens reveal that it shares synapomorphies with other crown-group hynobiids including the nasal anterior border notched for alary process of premaxilla, quadrate distally expanded, anteroventral process of orbitosphenoid present, three or less caudosacrals, and height of ossified scapular shorter than proximodistal length of coracoid (Jia, Anderson, and Gao 2021a). What is interesting is that the Anji Salamander has several more plesiomorphic and derived anatomical features that are ontogenetically and phylogenetically important for understanding the evolution of salamanders and even modern amphibians.

One unexpected discovery is that all specimens display a clearly-defined stapedial foramen that perforates the stylus of the stapes in posterior view of the skull (Figures 2 and 5). This discovery contradicts the previous statement that loss of the stapedial foramen is a synapomorphy of salamanders and anurans (Trueb and Cloutier 1991; Trueb 1993), and raises two major questions concerning the evolution of the stapes in salamanders: What other extant hynobiids may also possess a stapedial foramen but have not been documented in the literature, and how many times has the foramen been lost in salamanders?

As the sound-conducting ear ossicle occurring in amphibians, a stapes perforated by a foramen is a key structure in the origin and evolution of tetrapods (Clack and Anderson 2016), and consequently has received much attention in amphibians as the basal group of tetrapods (Kingsbury and Reed 1909; Monath 1965; Olson 1966; Clack and Anderson 2016; Schoch and Anderson 2016). The stapedial foramen functionally serves as the passage of the stapedial artery and/or the hyomandibular trunk of the facial nerve (CN VII) (Schmalhausen 1968), whereas impacts from the presence/absence of this foramen on hearing remains unknown.

In the fossil record, the stapedial foramen piercing the base of the stapes is found in most Paleozoic tetrapods including the earliest tetrapod *Acanthostega* and the ancestral group of lissamphibians (modern amphibians), temnospondyls (Clack and Anderson 2016; Schoch and Anderson 2016; Figure 5). In lissamphibians, a stapedial foramen is present in caecilians, the Jurassic stem-group salamander *Karaurus* (Ivachneneko 1978; Estes 1981), the Jurassic crown-group salamanders *Beiyanerpeton*, *Neimengtriton*, *Qinglongtriton* (Gao and Shubin 2012;

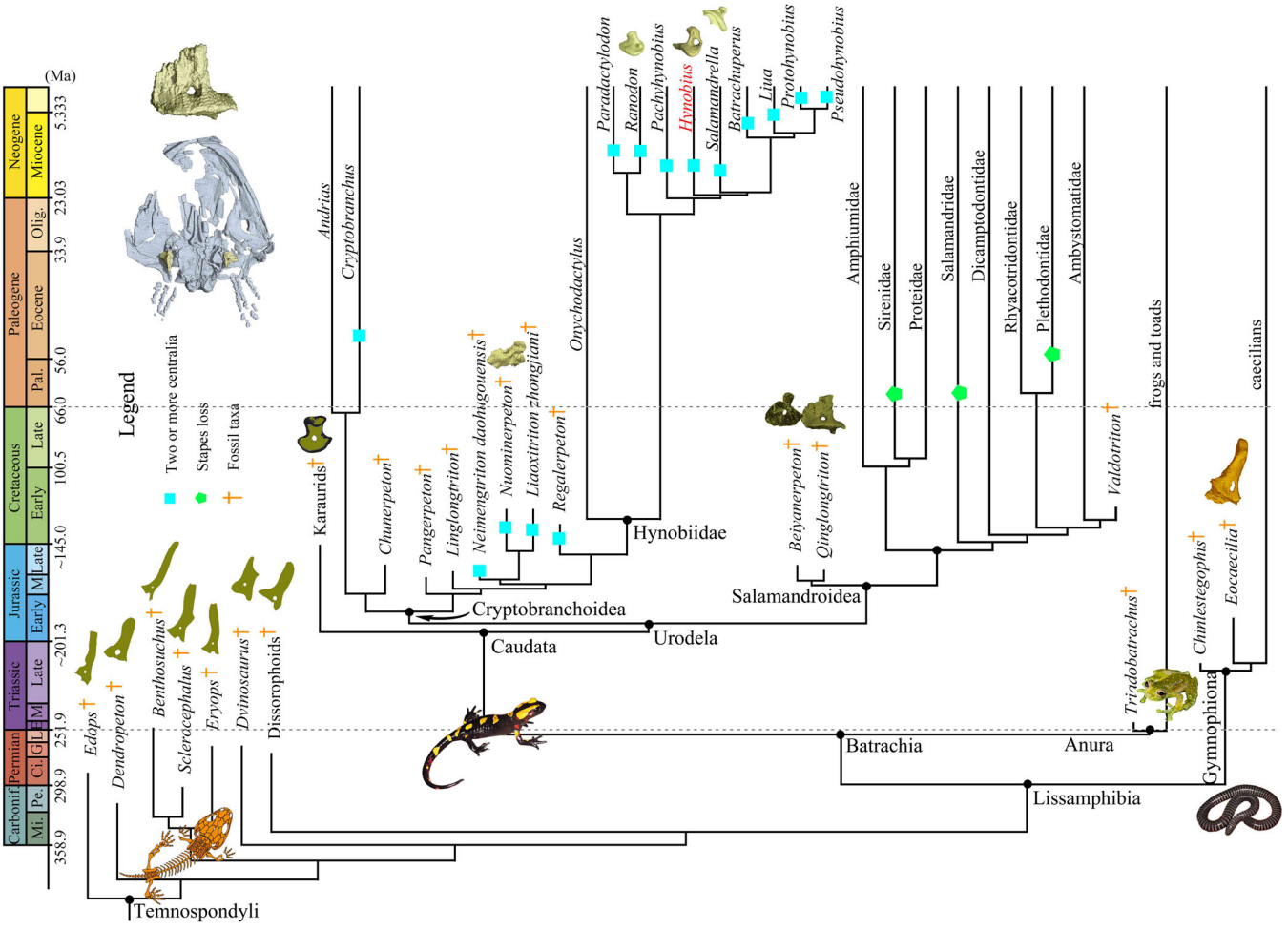

FIGURE 5 | Time-calibrated cladogram showing phylogenetic distribution of the possession of a stapedial foramen in the middle ear and the presence of two or more centralia in the mesopodium among fossil and living amphibian clades. Phylogenetic scheme based on Clack and Anderson (2016), Schoch and Anderson (2016), and Jia, Anderson and Gao (2021a).

Jia and Gao 2016; Jia, Anderson, and Gao 2021a), and is absent in anurans and living species of the advanced salamander clade Salamandroidea. In Salamandroidea, the stapes is even lost in Salamandridae and some species in Plethodontidae and Sirenidae (Rose 2003; Gao and Shubin 2012).

Although the literature on the amphibian ear is extensive, previous studies provided no evidence of the presence of a stapedial foramen in extant hynobiids (Monath 1965). In this regard, *Hynobius amjiensis* is so far the only living salamander species that unequivocally shows the presence of this foramen. Consistent occurrence of this foramen in all sampled specimens shows its significance in salamander phylogeny, unlike the individually variable conditions recently reported in some other hynobiid species (Jiang et al. 2018). Accumulating evidence from fossil and extant species suggests that salamanders primitively have a stapedial foramen inherited from the last common ancestor of modern amphibians, whereas mechanisms and patterns of independent losses of the foramen in salamanders and anurans remains an open question that deserves further investigation.

A second unexpected discovery is the procoracoid fused to the coracoid in the pectoral girdle and the pubis fused to the ischium in the pelvis. In most salamanders, the procoracoid and large parts of the coracoid remain cartilaginous in the adult (Shearman 2008), as does the pubis in the pelvis. In *Hynobius amjiensis*, post-metamorphic juveniles display the normal salamander ossification patterns of the pectoral and pelvic girdles (supplementary online material Figure S4). However, all breeding adults have the procoracoid and the coracoid partially ossified (Figure S5). By the same token, the pubis in the pelvis is ossified and completely fused with the ischium so that the paired obturator foramina are rimmed by the bony pubis and ischium (Figure 3). Recent studies have shown that the procoracoid and pubis are partially ossified in the stream hynobiids *B. londongensis* and *B. yenyuanensis* (Jiang et al. 2018; Jia et al. 2019), similar to the patterns of the girdle elements now known for *Hynobius amjiensis*, a terrestrial species. Therefore, the extra ossification and fusion of girdle elements can be recognized as noticeable developmental patterns associated with the post-metamorphic ontogeny of these species. Whether the extensive ossification in girdle elements in these derived hynobiids is related to ecological adaptation and phylogeny awaits to be tested with more thorough morphological investigations on hynobiids.

A third unexpected discovery concerns carpal and tarsal ossifications in hynobiids. Salamander limbs provide a source of information for addressing problems of morphological evolution (Shubin and Wake 2003). However, limb structures are poorly known for *Hynobius*. In this regard, our comparative studies of post-metamorphic juveniles with fully-grown adults provide valuable information concerning patterns of limb ossification in *Hynobius amjiensis*. No juvenile specimens show ossification of any carpal or tarsal elements (Figure S4). In contrast, breeding adults display complete or nearly complete ossification of the carpals in the manus and the tarsals in the pes, thereby showing that complete ossification of the carpals and tarsals is delayed after reaching sexual maturity (Figure S5).

Possession of two centralia in the carpus and tarsus has been recognized as a plesiomorphic condition in salamanders, and it has been documented for five (*Liua*, *Ranodon*, *Salamandrella*, *Batrachuperus*, *Paradactylodon*) out of the ten living genera in Hynobiidae (Shubin and Wake 2003), whereas the other four genera (*Hynobius*, *Onychodactylus*, *Pachyhynobius*, *Protohynobius*, *Psuedohynobius*) were thought to have a single centrale. Similarly, previous studies identified an unusual arrangement of carpals in the stream hynobiid *Batrachuperus*: a large proximal centrale is in direct contact with the radius, so that the centrale separates the radiale from the intermedium (Jiang et al. 2018; Jia et al. 2019; Shubin and Wake 2003). This is regarded as a plesiomorphic condition, not found in other living salamanders but present in basal tetrapods, such as temnospondyls (Shubin and Wake 2003). Interestingly, our findings of both the two centralia in the carpus and the presence of a centrale-radius contact in the Anji Salamander demonstrate plesiomorphic characters are more widely present in Hynobiidae as expected (Figure 4).

More interestingly, *Hynobius amjiensis* has no ossified postminimus in the pes, a derived condition within the advanced clade Salamandroidea. A postminimus is primitively present in six hynobiid genera (*Liua*, *Ranodon*, *Salamandrella*, *Onychodactylus*, *Batrachuperus*, *Paradactylodon*), and it is also known for the cryptobranchid genus *Andrias* but not its sister taxon *Cryptobranchus* (Shubin and Wake 2003). In this context, the Anji Salamanders appears to show a rare case among extant hynobiids with loss of the postminimus if confirmed with future studies on the absence of a cartilaginous postminimus. The mosaic pattern of primitive and derived characters in the skull and postcranial skeleton of *H. amjiensis* highlight that highly-nested taxa are indispensable in understanding of morphological evolutionary patterns of early salamanders.

5 | Conclusions

Over the past two decades, our understanding on the early evolution of salamanders has greatly benefited from both the many Mesozoic salamander discoveries mainly from China, and the osteological studies of the primitive living hynobiids endemic to eastern Asia. Our descriptions of the critically-endangered Anji Salamander (*Hynobius amjiensis*) find many unexpected atavistic features that are rarely seen in modern salamanders, including presence of a stapedial foramen at the base of stapes in the middle ear, presence of two centralia in the forelimb, and a direct bony contact between the proximal centrale and radius. On the other hand, the Anji Salamander has several derived characters that are potentially informative in phylogenic and developmental analyses, including the presence of extensive ossifications in both the pectoral and pelvic girdles and unlike most living hynobiids has no ossified postminimus in the pes. The consistent presence of both the atavistic and derived characters in all sampled specimens of *H. amjiensis* demonstrates that the deeply-nested, most specious, and yet poorly-studied genus of living hynobiids, *Hynobius*, is indispensable in advancing our knowledge of morphological evolutionary patterns of early salamanders. The last common ancestor of salamanders, frogs, and caecilians is expected to have a stapedial foramen, and what mechanisms drive the loss

of the foramen in modern anurans and salamanders is worthy to explore in the future.

Author Contributions

Cang-Song Chen: conceptualization, data curation, funding acquisition, investigation, resources, visualization, Writing—editing. **Jia Jia:** conceptualization, data curation, formal analysis, funding acquisition, investigation, methodology, resources, visualization, writing—original draft, writing—editing. **Xian-Ting Wang:** data curation, resources. **Jia Yang:** formal analysis, data curation, methodology, writing—editing. **Ke-Qin Gao:** conceptualization, funding acquisition, investigation, methodology, project administration, visualization, writing—original draft, writing—editing.

Acknowledgements

The authors thank Li-peng Yu (Longwangshan Nature Reserve) and Ze-dong Lang and Rui Guo for their help with arrangement for our visit to the type locality Longwangshan. We are grateful to Y. Peng (Zhejiang University) for helping with CT scanning of specimens and Professor RC Fox (University of Alberta) for improving the English. We thank Professors Jian-Piang Jiang and Bin Wang (Chengdu Institute of Biology) for access of specimens. This research was supported by the National Natural Science Foundation of China (NSFC 41872008, 41702002) and the Natural Science Foundation of Zhejiang (LTGS23C030003 and LGN19C040002).

Conflicts of Interest

The authors declare no conflicts of interest.

Data Availability Statement

The data that supports the findings of this study are available in the supplementary material of this article.

All specimens used in this study are reposited in the Zhejiang Museum of Natural History (ZMNH), Hangzhou, Zhejiang Province, China.

All data generated or analyzed during this study are included in this published article (and its electronic appendix files).

Peer Review

The peer review history for this article is available at https://www.webofscience.com/api/gateway/wos/peer-review/10.1002/jmor.70028.

References

AmphibiaWeb. 2024. *Information on Amphibian Biology and Conservation*. The University of California. Accessed August 15, 2024 http://amphibiaweb.org.

Ashley-Ross, M. A. 1992. "The Comparative Myology of the Thigh and Crus in the Salamanders *Ambystoma tigrinum* and *Dicamptodon tenebrosus*." *Journal of Morphology* 211: 147–163. https://doi.org/10.1002/jmor.1052110204.

Boisvert, C. A. 2009. "Vertebral Development of Modern Salamanders Provides Insights Into a Unique Event of Their Evolutionary History." *Journal of Experimental Zoology Part B: Molecular and Developmental Evolution* 312B: 1–29. https://doi.org/10.1002/jez.b.21238.

Cao, Z., R. Guo, Z. Fang, et al. 2024. "Normal Table of Embryonic Development in the Anji Salamander *Hynobius amjiensis* (Hynobiidae)." *Developmental Biology* 511: 84–91. https://doi.org/10.1016/j.ydbio.2024.04.005.

Carroll, R. L., and R. Holmes. 1980. "The Skull and Jaw Musculature as Guides to the Ancestry of Salamanders." *Zoological Journal of the Linnean Society* 68: 1–40. https://doi.org/10.1111/j.1096-3642.1980.tb01916.x.

Chen, C., J. Yang, Y. Wu, et al. 2016. "The Breeding Ecology of a Critically Endangered Salamander, *Hynobius amjiensis* (Caudata: Hynobiidae), Endemic to Eastern China." *Asian Herpetological Research* 7: 53–58. https://doi.org/10.16373/j.cnki.ahr.150050.

Chen, C. S., and J. Yang. 2012. "Habitat Monitoring of *Hynobius amjiensis* in Longwangshan, China." *National Wetland* 3: 86–91.

Chen, K. Y., R. Guo, L. Xia, Y. Y. Mei, C. S. Chen, and J. Yang. 2023. "Genome Survey and Characterization of New Microsatellite Markers in *Hynobius amjiensis* (Caudata: Hynobiidae)." *Salamandra* 59: 117–124.

Chen, M. Y., R. L. Mao, D. Liang, M. Kuro-o, X. M. Zeng, and P. Zhang. 2015. "A Reinvestigation of Phylogeny and Divergence Times of Hynobiidae (Amphibia, Caudata) Based on 29 Nuclear Genes." *Molecular Phylogenetics and Evolution* 83: 1–6. https://doi.org/10.1016/j.ympev.2014.10.010.

Clack, J. A., and J. S. Anderson. 2016. "Early Tetrapods: Experimenting With Form and Function." In *Evolution of the Vertebrate Ear*, edited by J. Clack, R. Fay, and A. Popper, 71–105. Springer. https://doi.org/10.1007/978-3-319-46661-3_4.

Cope, E. D. 1859. "On the Primary Divisions of the Salamandridae, With Descriptions of Two New Species." *Proceedings of the Academy of Natural Sciences of Philadelphia* 11: 122–128.

Duméril, A. M. C. 1806. Zoologie Analytique, ou *Méthode Naturelle de Classification des Animaux, Rendue plus Facile à l'aide de Tableaux Synoptiques*. Allais, libraire.

Dunn, E. R. 1922. "The Sound-Transmitting Apparatus of Salamanders and the Phylogeny of the Caudata." *American Naturalist* 56: 418–427. https://doi.org/10.1086/279882.

Estes, R. 1981. *Encyclopedia of Paleoherpetology, Part 2: Gymnophiona, Caudata*. Gustav Fischer Verlag.

Fei, L., and C. Ye. 2016. *Amphibians of China* (I). Science Press.

Francis, E. T. B. 1934. *The Anatomy of the Salamander*. Clarendon Press.

Fu, C., R. Rao, J. Wu, J. Chen, and G. Lei. 2003. "Effects of Density and Food Availability on Growth and Cannibalism in Basin-Raising Larval Salamanders (*Hynobius amjiensis*)." *Zoological Research* 24: 186–190.

Gao, K. Q., and N. H. Shubin. 2012. "Late Jurassic Salamandroid From Western Liaoning, China." *Proceedings of the National Academy of Sciences* 109: 5767–5772. https://doi.org/10.1073/pnas.1009828109.

Gregory, J. T., F. E. Peabody, and L. I. Price. 1956. "Revision of the Gymnarthridae American Permian Microsaurs." *Bulletin of the Peabody Museum of Natural History* 10: 1–77.

Gu, H. 1992. "A new species of *Hynobius-Hynobius amjiensis*." In Animal Science Research: A Symposium Issued to Celebrate the 90th Birthday of the Professor Mangven Ly Chang, edited by Y. Qian, E. Zhao, and K. Zhao, 39–43. China Forestry Press.

Gu, H., X. Mao, J. Wang, Z. Du, and X. Lou. 1999. "Research on Population Size and Dynamics of *Hynobius amjiensis*." *Sichuan Journal of Zoology* 18: 104–106.

Hara, S., and K. Nishikawa. 2021. "Osteological Characteristics of the Setouchi Salamander *Hynobius setouchi* (Urodela, Hynobiidae)." *Anatomical Record* 305: 1316–1342. https://doi.org/10.1002/ar.24789.

IUCN. (2007). The Red List of Threatened Species. http://www.iucnredlist.org.

IUCN. 2019. *The IUCN Red List of Threatened Species*. Version 2019-2. IUCN. https://www.iucnredlist.org.

IUCN SSC Amphibian Specialist Group. 2021. Hynobius amjiensis, e.T59089A63876823. The IUCN Red List of Threatened Species 2021. https://doi.org/10.2305/IUCN.UK.2021-3.RLTS.T59089A63876823.en.

Ivachneneko, M. 1978. "Urodeles From the Triassic and Jurassic of Soviet Central Asia." *Paleontological Journal* 1978: 362–368.

Jia, J., J. S. Anderson, and K. Q. Gao. 2021a. "Middle Jurassic Stem Hynobiids From China Shed Light on the Evolution of Basal Salamanders." *iScience* 24: 102744. https://doi.org/10.1016/j.isci.2021.102744.

Jia, J., J. S. Anderson, J. P. Jiang, W. Wu, N. H. Shubin, and K. Q. Gao. 2022. "Ossification Patterns of the Carpus and Tarsus in Salamanders and Impacts of Preaxial Dominance on the Fin-To-Limb Transition." *Science Advances* 8: eabq7669. https://doi.org/10.1126/sciadv.abq7669.

Jia, J., and K. Q. Gao. 2016. "A New Basal Salamandroid (Amphibia, Urodela) From the Late Jurassic of Qinglong, Hebei Province, China." *PLoS One* 11: e0153834. https://doi.org/10.1371/journal.pone.0153834.

Jia, J., K. Q. Gao, J. P. Jiang, G. S. Bever, R. Xiong, and G. Wei. 2021b. "Comparative Osteology of the Hynobiid Complex *Liua-Protohynobius-Pseudohynobius* (Amphibia, Urodela): I. Cranial Anatomy of *Pseudohynobius*." *Journal of Anatomy* 238: 219–248. https://doi.org/10.1111/joa.13311.

Jia, J., J. P. Jiang, M. H. Zhang, and K. Q. Gao. 2019. "Osteology of *Batrachuperus yenyuanensis* (Urodela, Hynobiidae), a High-Altitude Mountain Stream Salamander From Western China." *PLoS One* 14: e0211069. https://doi.org/10.1371/journal.pone.0211069.

Jiang, J., J. Jia, M. Zhang, and K. Q. Gao. 2018. "Osteology of *Batrachuperus londongensis* (Urodela, Hynobiidae): Study of Bony Anatomy of a Facultatively Neotenic Salamander from Mount Emei, Sichuan Province, China." *PeerJ* 6: e4517. https://doi.org/10.7717/peerj.4517.

Jiang, Z., J. Jiang, Y. Wang, et al. 2016. "Red List of China's Vertebrates." *Biodiversity Science* 24: 500–551.

Kingsbury, B. F., and H. D. Reed. 1908. "The Columella Auris in Amphibia." *The Anatomical Record* 2: 81–91.

Kingsbury, B. F., and H. D. Reed. 1909. "The Columella Auris in Amphibia. Second Contribution." *Journal of Morphology* 20: 549–628. https://doi.org/10.1002/jmor.1050200403.

Lapage, E. O. 1928. "The Septomaxillary. I. In the Amphibia Urodela." *Journal of Morphology* 45: 441–471. https://doi.org/10.1002/jmor.1050450203.

Li, Y. M., X. Y. Wu, G. F. Fang, C. M. Gu, H. Xue, and X. B. Wu. 2013. "*Hynobius amjiensis* Found in Anhui province, China." *Chinese Journal of Zoology* 48: 526–528.

Monath, T. 1965. "The Opercular Apparatus of Salamanders." *Journal of Morphology* 116: 149–170. https://doi.org/10.1002/jmor.1051160202.

Olson, E. C. 1966. "The Middle Ear—Morphological Types in Amphibians and Reptiles." *American Zoologist* 6: 399–419. https://doi.org/10.1093/icb/6.3.399.

Qiu, Y., K. Chen, Y. Mei, J. Yang, and C. Chen. 2024. "Pre-Embryonic Period Observation Shows a Unique Reproductive Strategy of the Critically Endangered Anji Salamander (*Hynobius amjiensis*)." *Animals: An Open Access Journal from MDPI* 14: 3007. https://doi.org/10.3390/ani14203007.

Rose, C. S. 2003. "The developmental morphology of salamander skull." In *Amphibian Biology*, edited by H. Heatwole and M. Davies, 5, 1684–1781. Surrey Beatty and Sons.

Sato, I. 1943. *A Monograph of the Tailed Batrachians of Japan*. Nippon Shuppan-Sha.

Schmalhausen, I. I. 1968. *The Origin of Terrestrial Vertebrates*. Academic Press.

Schoch, R. R., and J. S. Anderson. 2016. "Amphibia: A Case of Diversity and Convergence in the Auditory Region." In *Evolution of the Vertebrate Ear*, edited by J. Clack, R. Fay, and A. Popper, 327–355. Springer. https://doi.org/10.1007/978-3-319-46661-3_11.

Shearman, R. M. 2008. "Chondrogenesis and Ossification of the Lissamphibian Pectoral Girdle." *Journal of Morphology* 269: 479–495. https://doi.org/10.1002/jmor.10597.

Shubin, N. H., and D. B. Wake. 2003. "Morphological Variation, Development, and Evolution of the Limb Skeleton of Salamanders." In *Amphibian Biology*, edited by H. Heatwole and M. Davies, 5, 1782–1808. Surrey Beatty and Sons.

Sparreboom, M. 2014. *Salamanders of the Old World: The Salamanders of Europe, Asia and Northern Africa*. Zeist: KNNV Publishing.

Trueb, L., and R. Cloutier. 1991. "A Phylogenetic Investigation of the Inter- and Intrarelationships of the Lissamphibia (Amphibia: Temnospondyli)." In *Origins of the Higher Groups of Tetrapods*, edited by H. D. Schultze and L. Trueb, 223–313. Ithaca: Cornell University Press.

Trueb, L. 1993. "Patterns of Cranial Diversity among the Lissamphibia." In *The Skull, Volume 2: Patterns of Structural and Systematic Diversity*, edited by J. Hanken and B. K. Hall, 255–343. The University of Chicago Press.

Tschudi von, J. J.. 1838. *Classification der Batrachier mit Berücksichtigung der Fossilen Thiere Dieser Abtheilung der Reptilien*. Petitpierre.

Vassilieva, A., J. S. Lai, S. F. Yang, Y. H. Chang, and N. A. Poyarkov, Jr. 2015. "Development of the Bony Skeleton in the Taiwan Salamander, *Hynobius formosanus* Maki, 1922 (Caudata: Hynobiidae): Heterochronies and Reductions." *Vertebrate Zoology* 65: 117–130.

Wang, Z., S. N. Othman, Z. Qiu, et al. 2023. "An Isolated and Deeply Divergent *Hynobius* Species From Fujian, China." *Animals: An Open Access Journal from MDPI* 13: 1661. https://doi.org/10.3390/ani13101661.

Wilder, I. W. (1925). *The Morphology of Amphibian Metamorphosis*. Smith College, Northampton.

Xiong, J., X. Liu, and X. Zeng. 2011. "Discovery of an Internasal Bone in *Hynobius maoershanensis* (Urodela: Hynobiidae)." *Asian Herpetological Research* 2: 87–90. https://doi.org/10.3724/SP.J.1245.2011.00087.

Yang, J., C. S. Chen, S. H. Chen, et al. 2016. "Population Genetic Structure of Critically Endangered Salamander (*Hynobius amjiensis*) in China: Recommendations for Conservation." *Genetics and Molecular Research* 15: gmr-15027733.

Zhang, P., Y. Q. Chen, H. Zhou, et al. 2006. "Phylogeny, Evolution, and Biogeography of Asiatic Salamanders (Hynobiidae)." *Proceedings of the National Academy of Sciences* 103: 7360–7365. https://doi.org/10.1073/pnas.0602325103.

Supporting Information

Additional supporting information can be found online in the Supporting Information section.